Current Drive by Spheromak Injection into a Tokamak

M. R. Brown and P. M. Bellan
California Institute of Technology, Pasadena, California 91125
(Received 5 October 1989)

We report the first observation of current drive by injection of a spheromak plasma into a tokamak (Caltech ENCORE small research tokamak) due to the process of helicity injection. After an abrupt 30% increase, the tokamak current decays by a factor of 3 due to plasma cooling caused by the merging of the relatively cold spheromak with the tokamak. The tokamak density profile peaks sharply due to the injected spheromak plasma ($\bar{n}_e$ increases by a factor of 6) then becomes hollow, suggestive of an interchange instability.

PACS numbers: 52.55.Hc, 52.55.Fa

A spheromak is a force-free toroidal magnetofluid equilibrium having linked and comparable toroidal and poloidal magnetic fluxes and having no material linking the center of the torus.[1] Magnetic helicity is a measure of the linked flux and the formation and sustainment of spheromaks has been explained in terms of helicity injection.[2] It has been postulated[3] that since magnetic helicity is a scalar, additive, nearly conserved quantity in resistive MHD (even in the presence of turbulent tearing[4]), the merging of an externally injected spheromak with a tokamak will yield a tokamak of higher helicity content provided the initial spheromak and tokamak discharges had the same sign of helicity. Since helicity is related to field-aligned current and the tokamak toroidal field is fixed by external coils, a tokamak with higher helicity content has higher toroidal current. Several models[3,5,6] have been proposed to predict the mechanism whereby an injected spheromak would slow down and be trapped within a tokamak discharge thereby depositing helicity and density, but until now there has been no experimental verification of the concept.

We report here the first experimental demonstration of tokamak current drive by spheromak injection into the tokamak. The experiment (see Fig. 1) was performed on Caltech's ENCORE tokamak ($R=0.38$ m, $a=0.12$ m, $I_p=2$ kA, $B_{\rm tor}=700$ G) with a spheromak ($r=0.04$ m, $\Phi_{\rm gun}=0.4$ mWb, $I_{\rm gun}=80$ kA) injected by a magnetized coaxial plasma gun. The injection of a spheromak results in a number of phenomena. (1) We observe an initial 30% increase in tokamak plasma current (from 2.0 to 2.6 kA) upon injection of a spheromak *only when both spheromak and tokamak have the same sign of helicity* [where the sign of helicity is defined as positive (right handed) if current flows parallel to magnetic field and negative (left handed) if antiparallel]. Increases in tokamak current of over 1 kA have been measured with high-energy spheromaks but these shots abruptly terminate the tokamak discharge. If the spheromak and tokamak have different signs of helicity, the tokamak current drops by about 20%. The initial increase (decrease) in current is accompanied by a sharp decrease (increase) in loop voltage and the tokamak helicity increase is consistent with the helicity content of the injected spheromak. (2) After the initial increase ($\cong 30$ μs after injection) we observe a decline in current to a lower level due to a sudden cooling of the tokamak plasma from 12 to 4 eV and the addition of impurities. (3) We observe an increase in the tokamak central density by a factor of 6. The density of profile becomes peaked and is followed by what appears to be an interchange instability which flattens the profile. (4) Measurements of the transient magnetic fields in the tokamak discharge indicate that the spheromak tilts in the cylindrical entrance region and remains with its magnetic moment oriented *antiparallel* to the toroidal field of the tokamak (opposite that expected for a rigid magnetic dipole).

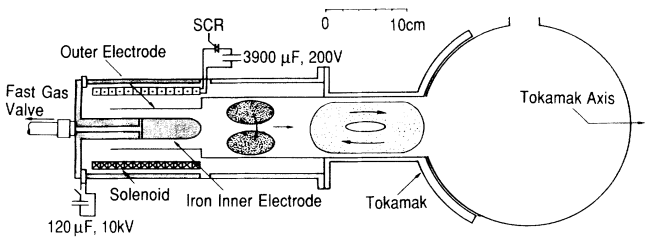

FIG. 1. Schematic of experimental setup showing topology of injected spheromak.

The spheromak is formed by a coaxial, magnetized plasma gun similar in design to those used by Alfvén *et al.*[7] (Fig. 1). The center electrode of the gun and an outer yoke (constructed of high-permeability cold-rolled steel and Monel) form a magnetic circuit. The center electrode is 2.5 cm in diameter, the outer electrode is 5.1 cm in diameter, and the cylindrical entrance region is 7.6 cm in diameter. A slow (2-ms rise time), low-energy (100 J) capacitor bank is used to energize a solenoid which provides the gun flux $\Phi_{\rm gun}$ at the tip of the center electrode (up to 1 mWb). A gas puff from a fast acting solenoid valve[8] provides a peak pressure in the gun breech of about 0.1 Torr (about 1 $\rm cm^3$atm hydrogen). This gas is fully ionized by the discharge current. We use a 10-kV, 6-kJ fast (10-μs rise time) capacitor bank to break down the gas in the gun and from a radial current sheet between the inner and outer electrodes. An axial $\mathbf{J}\times\mathbf{B}$ force accelerates the current sheet along the gun barrel until the plasma reaches the magnetic flux at

the gun muzzle. If the $\mathbf{J}\times\mathbf{B}$ force is strong enough to overcome the magnetic tension at the gun muzzle, then a free spheromak forms and propagates away from the gun. As sketched in Fig. 1, the spheromak is observed (using magnetic probes) to tilt in the entrance region.

We typically operate with $\Phi_{gun}=0.3$–0.5 mWb and discharge current, $I_{gun}=60$–120 kA, with a 3.5–7-kV charge on the capacitor. We have found it is necessary to operate above a gun threshold, $\lambda_{th}=\mu_0 I_{gun}/\Phi_{gun}\cong 250$ m^{-1}, otherwise a free spheromak is not formed (Barnes *et al.*[2] have made similar observations on the CTX spheromak). The spheromak moves from the gun to the tokamak at the local Alfvén velocity (about 3×10^4 m/s). Typical spheromak densities and temperatures are 10^{21} m^{-3} and 7 eV as measured by a double Langmuir probe in the tokamak vessel directly in front of the gun. The density measurements have been corroborated with a 3-mm density interferometer (on the opposite side of the tokamak chamber). The tokamak vessel volume is about a factor of 100 larger than the initial spheromak volume and we measure peak densities of about 10^{19} m^{-3} with the interferometer. Temperature measurements have been corroborated by a measurement of ratio of C IV (253 nm) to C III (230 nm) line emission[9] and are consistent with those calculated from resistive decay times (assuming Spitzer resistivity and $Z_{eff}\cong 2$–4).

We are able to generate spheromak and tokamak discharges of either helicity sign. We reverse the helicity sign of the spheromak by changing the direction of the gun flux Φ_{gun} and we reverse the sign of the tokamak by reversing the direction of the toroidal field. Figures 2 and 3 show our helicity injection results with all combinations of helicity sign. In Fig. 2, curves *a* and *c*, we show the tokamak plasma current I_p with injection of a spheromak into a tokamak discharge of the same sign (left into left and right into right, respectively), while in Fig. 2, curves *b* and *d*, we show the effect of injecting a spheromak into a tokamak of opposite sign (left into right and right into left, respectively). Note that we are able to change the sign of tokamak and spheromak helicity independently and have found an increase in I_p (i.e., helicity) *only* when both tokamak and spheromak have the same helicity sign. When the tokamak and spheromak have opposite helicity sign, there is a sharp decrease in I_p upon spheromak injection. To check possible interaction with the external Ohmic heating (OH) power supply, we monitored the current change ΔI_{OH} in the OH transformer primary during injection of a high-

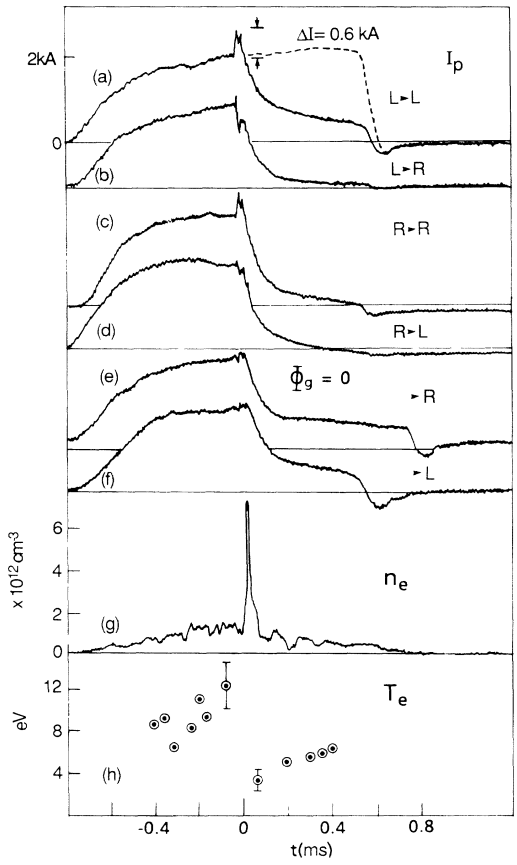

FIG. 2. Time histories of tokamak discharge ($B_\phi=700$ G) with spheromak injection ($I_{gun}=80$ kA, $\Phi_{gun}=0.4$ mWb), time scale relative to injection, each trace is a single shot, curve *a*, I_p with left-handed spheromak injected into a left-handed tokamak (dashed line is normal shot without spheromak injection); curve *b*, left into right; curve *c*, right into right; curve *d*, right into left; curve *e*, Marshall gun ($\Phi_{gun}\cong 0$) into left and, curve *f*, right; curve *g*, electron density; and curve *h*, temperature traces from Langmuir probe.

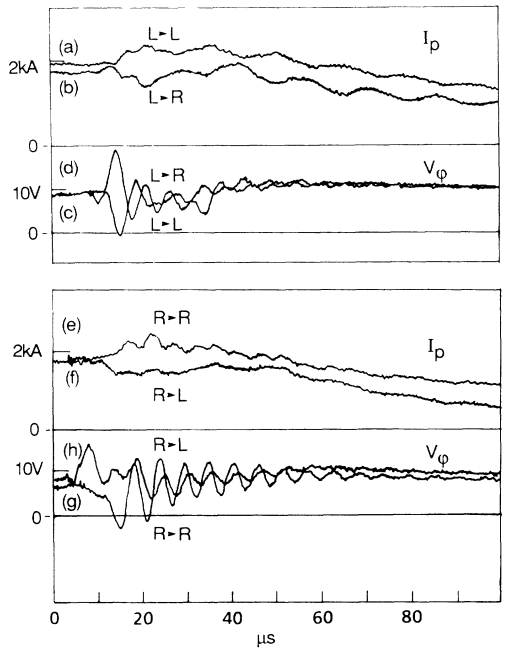

FIG. 3. Plasma current and loop voltage of Fig. 2, curves *a*–*d*, with time scale expanded, curves *a* and *c*, left → left; curves *b* and *d*, left → right; curves *e* and *g*, right → right; curves *f* and *h*, right → left.

energy spheromak and observed $\Delta I_{OH} < 160$ A turn when $\Delta I_p \cong 1100$ A. Thus, the sudden increase in I_p cannot be due to ΔI_{OH}. We have repeated the experiment with the Rogowski coil at four different toroidal locations spaced around the machine and have found that the measured ΔI_p is independent of toroidal location. If the gun flux is disabled and we inject a stream of plasma (Marshall gun injection[10]), we observe the same density increase as with finite Φ_{gun} but no ΔI_p (as expected, Fig. 2, curves *e* and *f*). Similarly, if we fire the gun below the threshold (I_{gun} not large enough to overcome Φ_{gun}), no ΔI_p or density increase is observed.

Note that the injected spheromak raises the central density from about 1×10^{12} to 6×10^{12} cm^{-3} (Fig. 2, curve *g*) but the high-density and high-current discharge persists for less than 100 μs (a few particle confinement times). Evidently this is because the tokamak magnetic pressure is unable to support the additional plasma pressure (i.e., a density or β limit is exceeded). After the initial helicity injection effect (increase or decrease depending on the signs), I_p decays by about a factor of 3. Langmuir-probe measurements of the electron temperature ($\frac{1}{4}$ circumference away from the injection point) show that the tokamak temperature slowly increases (due to Ohmic heating) to $\cong 12$ eV just before spheromak injection and then sharply drops to $\cong 4$ eV just after (Fig. 2, curve *h*). The calculated L/R decay time of I_p due to cooling is $\cong 70$ μs (for $L_{tok} \cong 0.5$ μH and $R_{tok} \cong 7$ mΩ assuming Spitzer resistivity with $Z=2$ and $T_e = 4$ eV) which is about the observed value. Measurements of the tokamak line emission show a more than a factor of 10 increase in H α emission upon spheromak injection and little increase in impurity line emission.[9] Firing the gas valve alone without firing the gun has no effect on tokamak plasma density or I_p since the slow moving neutral gas does not reach the tokamak vessel until after the shot is terminated.

Having demonstrated that the observed current drive effect has the expected sign for helicity injection [increase (decrease) in I_p if spheromak and tokamak have the same (opposite) helicity sign], we now estimate the magnitude of spheromak helicity in order to compare to the observed increase in tokamak helicity. The helicity content of the injected spheromak can be estimated a number of ways.

(i) First, the formal definition ($K = \int \mathbf{A}\cdot\mathbf{B}\, d^3x$) can be approximated by $K_{sph} \cong \alpha \Phi_{tor}\Phi_{pol}$, where α is a constant of order unity. For the case of two separate, discrete linked fluxes[2] $\alpha = 2$; for the case of an axisymmetric spheromak in a cylindrical flux conserver,[11] α is close to unity. The helicity content of the spheromak that ultimately moves into the tokamak is estimated from measurements performed on the spheromak in the tokamak vessel without tokamak plasma. We can therefore estimate

$$K_{sph} \cong \Phi_{tor}\Phi_{pol} \cong (B_{avg}Lr)(B_{avg}\pi r^2/4) \cong B_{avg}^2 \pi L r^3/4,$$

where B_{avg} is the volume-averaged magnetic field measured in the spheromak equilibrium, L is its length, and r is the radius of the cylindrical flux conserver (the tokamak minor radius in this case). From extensive magnetic-probe measurements performed in the tokamak vacuum vessel[12] we typically find $B_{avg} \cong 200$ G, $r = 0.12$ m, and $L \cong 4r$ so that $K_{sph} = 3\times10^{-7}$ Wb^2.

(ii) Second, we may also make this estimate by noting[2] that the energy per unit helicity of the spheromak equilibrium is $2\mu_0 W_{mag}/K_{sph} = \lambda_{eq}$ [where $W_{mag} = (B_{avg}^2/2\mu_0)\pi r^2 L$ is the spheromak magnetic energy and λ_{eq} is the eigenvalue of the equation of the force-free state, $\nabla\times\mathbf{B} = \lambda_{eq}B$]. Again, for an axisymmetric spheromak in a cylindrical flux conserver we have[13] $\lambda_{eq} = (k_z^2 + k_r^2)^{1/2}$, where $k_z = \pi/L$ and $k_r = 3.83/r$. From the measurements discussed above, we find $\lambda_{eq} = 32$ m^{-1} from which we obtain the same result $K_{sph} = 3\times10^{-7}$ Wb^2 (more careful calculations of λ_{eq} from a fit of data to a simple model[12] yield a similar result).

(iii) Third, we may estimate the helicity content of the spheromak by first noting that helicity is generated by the coaxial magnetized plasma gun at a rate[2] $\dot{K} = 2V_{gun}\Phi_{gun}$, where V_{gun} is the voltage that develops between inner and outer electrodes. Note that V_{gun} is determined by dynamic gun impedance and is usually significantly less than the voltage on the capacitor bank. We find that $K_{initial} \cong \int 2V_{gun}\Phi_{gun}\, dt \cong 4\times10^{-6}$ Wb^2 for typical values of $V_{gun} = 1$ kV, $\Phi_{gun} = 0.4$ mWb, and the duration the voltage is applied $\Delta t \cong 5$ μs. We make the further observations that (1) the magnetic *e*-folding time of our spheromaks is 10 μs so that the helicity decay time, $\tau_K \cong \tau_B/2$, is about 5 μs and (2) that the velocity of our spheromaks is about 3 cm/μs. We may infer, then, that initial helicity content of our spheromak decays about two *e*-folding times while traversing the 30 cm between gun and tokamak (the helicity injection effect was not observed in other experiments[9] where the helicity decay time was 20% shorter, due to impurities from plastic rather than ceramic insulators). We find by this calculation $K_{sph} = 5\times10^{-7}$ Wb^2, consistent with the other two methods.

Finally, the increase in tokamak helicity can be estimated by $K_{tok} \cong \Phi_{tor}\Phi_{pol}$, so we obtain (for a uniform current distribution) $\Delta K_{tok} \cong \mu_0\pi B_{tor}\Delta I_p a^2 R/2 \cong 4.5\times10^{-7}$ Wb^2 for $\Delta I_p = 600$ A and $B_{tor} = 700$ G. We conclude that the increase in tokamak helicity is consistent with the helicity of the injected spheromak estimated above.

Figure 3 depicts I_p and loop voltage on an expanded time scale for each of the four combinations of spheromak and tokamak helicity sign. Here again we observe the helicity injection effect only when both discharges have the same sign. Note also that the loop voltage drops (increases) as I_p increases (drops). The change in loop voltage is consistent with the change in I_p; $V_{loop} = L\, dI_p/dt$ and $L_{tok} \cong 0.5$ μH while $dI/dt \simeq (600$ A$)/(10$ μs) which gives a voltage ($\Delta V_{loop} \cong 30$ V) within

a factor of 3 of the measured value. The oscillations in the I_p trace appear to be due to Alfvénic disturbances (where the oscillation period is the toroidal transit time at the Alfvén speed). We have observed a magnetic pulse moving away from the spheromak injection point at $\cong 15$ cm/μs (which corresponds to a 16-μs transit time around the machine). The fact that the oscillations in the loop voltage are at about twice the frequency of those in I_p suggests a nonlinear coupling between I_p and inductance upon spheromak injection [where $V_{\text{loop}} = d(L_{\text{tok}} I_p)/dt$ and both L_{tok} and I_p have oscillatory parts].

A Langmuir-probe array measured the tokamak density profile at four minor radial positions during spheromak injection. The array was located $\frac{1}{4}$ of the tokamak circumference away from the spheromak injection point. A typical sequence is depicted in Fig. 4. Before spheromak injection (-30 μs) the tokamak density profile is relatively flat (Fig. 4, curve *a*). The injected spheromak increases the tokamak central density (at $+70$ μs) and sharply peaks the profile (Fig. 4, curve *b*). The profile then becomes hollow suggestive of a pressure-gradient-induced interchange instability[14] at $+90$ μs (Fig. 4, curve *c*). Finally, the profile returns to a less peaked configuration about 140 μs after injection (Fig. 4, curve *d*). The radial electron temperature profile remains relatively flat. Injection of the spheromak into the empty tokamak vacuum vessel results in a monotonic density profile that decays self-similarly in time.

Each of the theories relevant to spheromak injection into tokamaks[5,6] has predicted that the kinetic-energy density of the spheromak $\rho v_{\text{sph}}^2/2$ must exceed the magnetic energy density of the tokamak $B_{\text{tok}}^2/2\mu_0$ for the spheromak to penetrate the tokamak fields. In our case, v_{sph} is just the spheromak Alfvén speed (since we do not employ a separate acceleration stage) so the above condition reduces to $B_{\text{sph}} > B_{\text{tok}}$. We have verified that the spheromak does not penetrate the tokamak toroidal vacuum fields unless this condition is met.[12] Measurements of the fluctuating magnetic fields in the tokamak discharge after spheromak injection indicate[12] that the spheromak remains antialigned to the tokamak toroidal field contrary to the Perkins model.[5]

There are three further issues that we can address with our experimental results. First, it appears that in our experiment, the external torque due to the interaction of spheromak magnetic moment with tokamak fields[5] is dominated by internal MHD tilting. This is expected if $B_{\text{sph}} > B_{\text{tok}}$ since the time scale for an internal MHD tilt is an internal Alfvén time ($\sim B_{\text{sph}}^{-1}$) whereas the time scale for an external torque varies according to $\sim (B_{\text{sph}} B_{\text{tok}})^{-1/2}$. Second, we observe spheromak expansion along tokamak field lines but it appears that pressure balance in our case is maintained by the walls and not the tokamak plasma.[5,6] Third, it appears that the Alfvén-wake drag mechanism postulated by Parks[6] is weak in our experiment [the stopping time due to this effect is roughly $t_{\text{stop}} \cong t_{\text{Alf}} (n_{\text{sph}}/n_{\text{tok}})^{1/2}$ which is longer than a spheromak lifetime in our case].

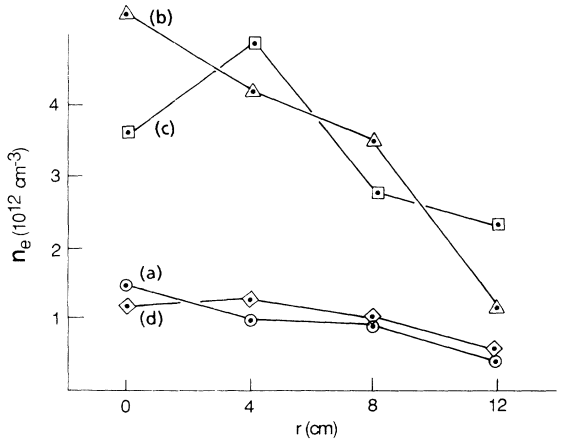

FIG. 4. Radial density profile (from Langmuir-probe array) before injection (curve *a*, -30 μs) and after injection (curve *b*, $+70$ μs; curve *c*, $+90$ μs; curve *d*, $+140$ μs).

In summary, small spheromaks injected into Caltech's ENCORE tokamak have been shown to drive plasma current (via helicity injection) as well as substantially increase tokamak density. Central densities have increased by a factor of 6 while plasma currents have been increased by 30% initially, followed by a reduction by a factor of 3. The spheromak tilts once and remains antialigned with the tokamak toroidal field.

This work was performed under DOE Grant No. DE-FG03-86ER53232. M.R.B. is a U.S. DOE Fusion Energy Postdoctoral Research Fellow.

[1]M. N. Rosenbluth and M. N. Bussac, Nucl. Fusion **19**, 489 (1979).

[2]C. W. Barnes *et al.*, Phys. Fluids **29**, 3415 (1986).

[3]C. W. Hartman and J. H. Hammer, Phys. Rev. Lett. **48**, 929 (1982).

[4]J. B. Taylor, Rev. Mod. Phys. **58**, 741 (1986).

[5]L. J. Perkins *et al.*, Nucl. Fusion **28**, 1365 (1988).

[6]P. B. Parks, Phys. Rev. Lett. **61**, 1364 (1988).

[7]H. Alfvén *et al.*, J. Nucl. Energy, Part C **1**, 116 (1960).

[8]Kindly provided by I. Henins, Los Alamos National Laboratory.

[9]M. R. Brown, A. D. Bailey, and P. M. Bellan (to be published).

[10]A. W. Leonard *et al.*, Phys. Rev. Lett. **57**, 333 (1986).

[11]W. C. Turner *et al.*, Phys. Fluids **26**, 1965 (1983).

[12]M. R. Brown, D. M. Cutrer, and P. M. Bellan (to be published).

[13]A. Bondeson *et al.*, Phys. Fluids **24**, 1682 (1981).

[14]F. J. Wysocki *et al.*, Phys. Rev. Lett. **61**, 2457 (1988).

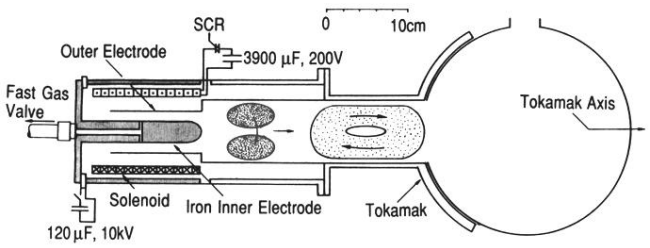

FIG. 1. Schematic of experimental setup showing topology of injected spheromak.